



Open Archive Toulouse Archive Ouverte (OATAO)

OATAO is an open access repository that collects the work of Toulouse researchers and makes it freely available over the web where possible.

This is a publisher-deposited version published in: <http://oatao.univ-toulouse.fr/>
Eprints ID: 4760

To link to this article: DOI:10.1063/1.3463400

URL: <http://dx.doi.org/10.1063/1.3463400>

To cite this version: Sendova, Mariana and Flahaut, Emmanuel and Hartsfield, Thomas (2010) *Temperature dependence of Raman scattering in filled double-walled carbon nanotubes*. Journal of Applied Physics, vol. 108 (n°4). ISSN 0021-8979

Any correspondence concerning this service should be sent to the repository administrator:
staff-oatao@inp-toulouse.fr

Temperature dependence of Raman scattering in filled double-walled carbon nanotubes

Mariana Sendova,^{1,a)} Emmanuel Flahaut,^{2,3} and Thomas Hartsfield¹

¹*New College of Florida, Sarasota, Florida 34243, USA*

²*Université de Toulouse, UPS, INP, Institut Carnot Cirimat, 118, route de Narbonne, F-31062 Toulouse Cedex 9, France*

³*CNRS, Institut Carnot Cirimat, F-31062 Toulouse, France*

(Received 7 May 2010; accepted 14 June 2010; published online 20 August 2010)

Four types of filled double-walled carbon nanotubes (DWNTs) (Se@DWNT; Te@DWNT; HgTe@DWNT; and PbI₂@DWNT) have been studied by high-resolution transmission electron microscopy and micro-Raman spectroscopy in the temperature interval from 80 to 700 K employing 785 nm excitation wavelength. The temperature dependence of the dominant bands (D-band, G-band, and the (2D)-band) are analyzed in terms of the model developed by Klemens, Hart, Agraval, Lax, and Cowley and extended by Balkanski for anharmonic decay of optical phonons. The quasi-harmonic frequencies and the anharmonicity constants were obtained from the temperature dependences of the analyzed Raman bands. The findings were compared to analogous study for empty DWNTs. The strength of the van der Waals interaction between the guest material and the carbon nanotube (CNT) estimated through the quasi-harmonic frequencies was found to decrease in the following order: Se@DWNT; Te@DWNT; PbI₂@DWNT, and HgTe@DWNT. In agreement with this, the anharmonicity due to the phonon-phonon interactions was found to decrease in the same order. © 2010 American Institute of Physics. [doi:10.1063/1.3463400]

I. INTRODUCTION

The synthesis of monodimensional nanocrystals is complex due to the lack of stability of such structures. One way to stabilize them is to prepare them within a container, such as a carbon nanotubes (CNTs) due to their inner diameter in the nanometer range, as well as their good chemical and thermal stability. The question which we attempt to answer with this study is what are the forces between the carbon atoms of the CNT walls and the atoms of the filling material. The aim of this work is to use temperature controlled micro-Raman spectroscopy to investigate how the presence of filling materials can modify the optical phonons decay mechanisms due to the additional van der Waals interactions between the nanotube walls and the guest materials. Earlier studies have revealed that the space available within CNT along with the van der Waals interactions with the tube walls may play an important role on the crystal structure of the confined material, especially in the case of narrow double-walled carbon nanotube (DWNT) where materials are often found in amorphous state even if they crystallize in single-walled CNT (SWNTs) of similar inner diameter.^{1,2} In this work we report the filling of DWNT by Se, Te, PbI₂, and HgTe using a capillary effect technique with melted filling materials, and their characterization by micro-Raman spectroscopy in the temperature range between 80 and 700 K.

II. EXPERIMENTAL

DWNT were synthesized by catalytic chemical vapor deposition as described in a previous paper.³ They were filled

using a high filling yield capillary wetting technique.¹ DWNT were mixed and gently ground together with the corresponding compound or element using a mortar and pestle (PbI₂ powder, 99.999% purity, Aldrich; Se powder, 99.999% purity, Aldrich; Te powder, 99.999% purity, Strem Chemicals; and HgTe powder, 99.9% purity, Strem Chemicals). The mixture was vacuum-sealed in a quartz ampoule which was heated in a programmed furnace at 5 K min⁻¹ to a temperature higher than the melting point of the filling material [PbI₂: 723 K (MP=681 K); Se: 573 K (MP=494 K); Te: 843 K (MP=722 K); and HgTe: 1000 K (MP=943 K)] with a dwell at this temperature (PbI₂: 5 h; Se: 24 h; Te: 10 h; and HgTe: 6 h) followed by cooling first ~100 K below the melting point at 0.1 K/min and then to room temperature at 1 K/min. In the case of PbI₂ (Ref. 1) and Se,⁴ the excess filling material contaminating the outside of the DWNT could be removed by washing at room temperature for a few minutes (PbI₂: 6M NaOH; Se: concentration HNO₃). In the case of Te (Ref. 5) and HgTe, because of the impossibility to dissolve them due to their very low solubility in acids, excess material located around the DWNT could not be removed. In most cases, the filling yield was roughly estimated to be ~50%, straight from high resolution transmission electron microscopy (HRTEM) observation. Figure 1 shows typical HRTEM images of the HgTe@DWNT sample of both bundles and individual nanotubes [Figs. 1(b), 1(d), and 1(f)], mostly filled along the whole observed length.

Raman spectra were acquired using a Leica DMLP microscope coupled to a Raman system manufactured by Kaiser Optical Systems Inc. The RamanRxn1™ analyzer incorporates the thermoelectrically (TE)-cooled charge coupled device detector for maximum sensitivity, Invictus™ near infrared (NIR) semiconductor laser with wavelength of 785 nm

^{a)}Electronic mail: sendova@ncf.edu.

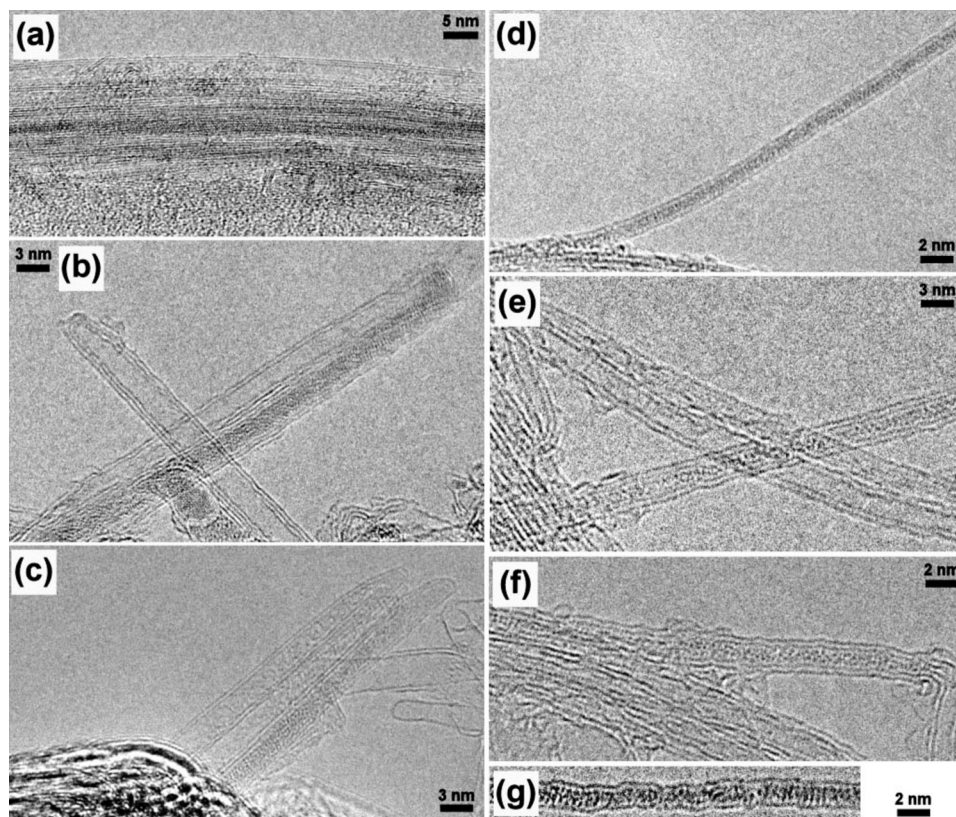


FIG. 1. HRTEM images of the HgTe@DWNT sample of both bundles and individual nanotubes.

(1.58 eV), and holographic grating to provide fast, simultaneous full spectral collection of Raman data. The spectral resolution in this Raman system is about 5 cm^{-1} . The laser spot diameter on the sample was $10 \text{ }\mu\text{m}$.

The power density was maintained at $13 \text{ }\mu\text{W}/\mu\text{m}^2$. Heating effects from the laser irradiation were considered negligible for 785 nm excitation wavelength at this power density level.⁶ The samples were heated in a Linkam THMS 600 heating stage in static air from 80 to 700 K. At each data point, the sample was left to thermalize for 15 min. Extreme care was taken to assure identical position of the laser spot at each temperature point. All spectra were normalized to the peak intensity of the strongest band in the spectra (G-band). All the numerical manipulations of the spectra were performed with GRAMS/AL 7.02 (Thermo Electron Corporation) and ORIGINPRO (Origin Laboratory Corporation) software.

III. RESULTS AND DISCUSSION

From the field emission gun scanning electron microscope images³ of raw nanotube powders, and taking into account the average length of the nanotubes, it was estimated that under the Raman microscope objective the sample from which the spectra were collected consisted of approximately 300 DWNTs. From HRTEM DWNT diameter distribution study conducted earlier³ it was estimated that the studied samples had approximately the following composition in terms of tube diameter for the inner tubes: (nanotubes number/diameter) 15/0.5 nm; $\approx 110/1.0 \text{ nm}$; $\approx 120/1.5 \text{ nm}$; $\approx 45/2.0 \text{ nm}$; and for the outer tubes: $\approx 10/1.0 \text{ nm}$; $\approx 60/1.5 \text{ nm}$; $\approx 120/2.0 \text{ nm}$, $\approx 110/2.5 \text{ nm}$. The energy of the excita-

tion photons used in our experiment is 1.58 eV. According to the Kataura plot⁷ SWNTs in resonance at this excitation wavelength are those with diameters between 0.9 nm and 2.0 nm giving rise to radial breathing modes (RBMs) between 120 and 300 cm^{-1} . The two dominant RBM bands in all of the CNTs used in this study are at 115 and 264 cm^{-1} , which are in good agreement with the Raman shifts predicted for 0.94 and 1.63 nm semiconducting CNTs, in agreement with the E_{33}^s and E_{22}^s electronic transitions.

The G-band is the most intense Raman spectral feature ($1550\text{--}1600 \text{ cm}^{-1}$). It is a result of tangential C–C bond stretching. Symmetry assignments of four Lorentzian components of the G-band [$\sim 1549(\omega_{E_2}^-)$, $\sim 1567(\omega_G^-)$, $\sim 1590(\omega_G^+)$, and $\sim 1607(\omega_{E_2}^+)$] cm^{-1} of single semiconducting SWNT have been reported.⁸ For comparative reasons, we analyzed the G-band of the DWNT powder samples by fitting it with the minimum number of Lorentzian line shapes, in this case four, in the range from 1500 to 1660 cm^{-1} . Figure 2 compares the quality of the fit of the G-band at 80 K. The four components are labeled L1 to L4 in order of increasing Raman shift. The dominant Lorentzian line shapes from the G-band are L3 and L4. The integral intensity of L3, $I(L3)$ is between 50% and 60% of the overall integral intensity of the G-band, $I(G)$. L3 might have contributions from the graphitelike (1580 cm^{-1}) line and from the ω_G^+ mode. $I(L4)$ is between 10% and 30% of $I(G)$. Each one of the other two components, L1 and L2, has less than 10% contribution. Position, ω , full width at half maximum (FWHM) Γ , and the ratio of $I(L3)/I(L4)$ for each type of filled DWNTs are summarized in Table I. The uncertainty from the fitting proce-

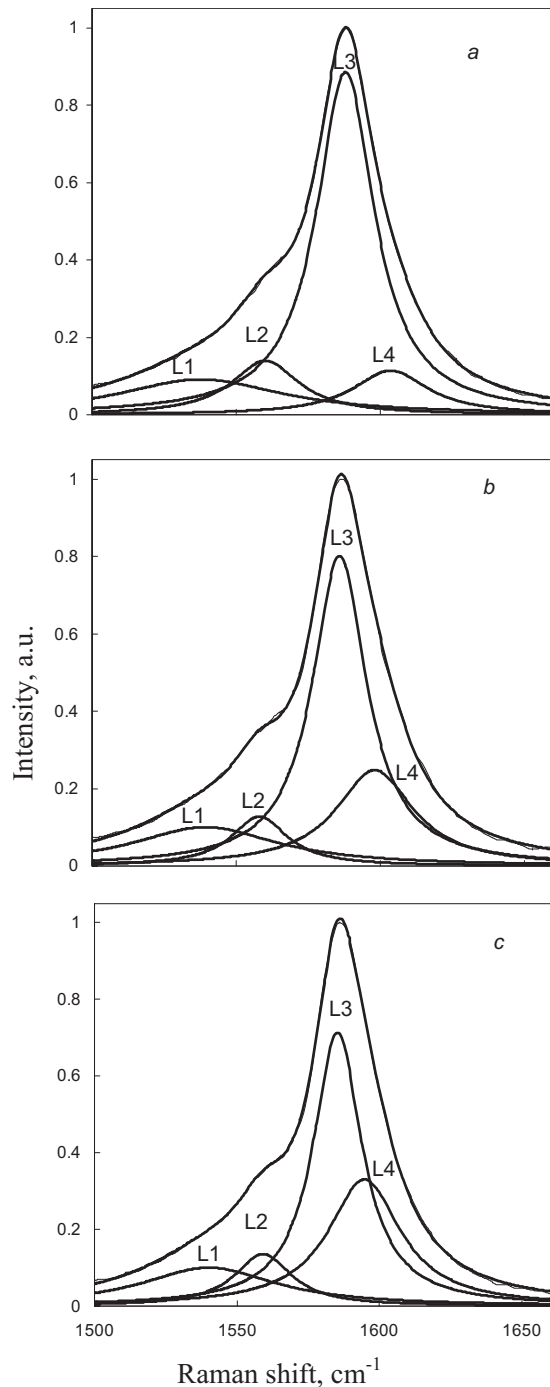


FIG. 2. G-band at 80 K fitted by four Lorentzian line shapes (a) Se@DWNT; (b) PbI₂@DWNT; and (c) empty DWNT.

cedure in determining the peak position of the most intense components is not more than 1 cm⁻¹. The main component, L3, in the G-band does not exhibit change in the FWHM depending on the filling material, Table I. The main difference between the filled DWNT G-band at 80 K is in the L4, L3 intensity ratio, and their separation. It seems that according to these two criteria the samples can be divided into two groups: Se@DWNT and Te@DWNT being in one group with L3 L4 peak separation of around 16 cm⁻¹ and integral intensity ratio around 6; and PbI₂@DWNT and HgTe@DWNT constituting another group characterized by smaller separation around 12 cm⁻¹ and integral intensity ratio of around 3. As compared to the empty DWNT samples which have a L3 L4 peak separation of around 10 cm⁻¹ and I(L3)/I(L4) is only 1.5. According to previous publications⁸ $\omega_{E_2}^+$ mode which in our case can be associated with L4, is coming mostly from nanotubes with high chiral angles. L4 decreases in relative intensity from the empty DWNT to Se@DWNT. This might be interpreted as an indication of chirality (or electronic density of states) induced change from the presence of the filling material, caused by the tube-filling material van der Waals interaction. DWNTs which have been in resonance with the excitation photons in the empty DWNT are not in resonance once the filling atoms were introduced. From the band fit it can be suggested that the dominant G-band component (L3) in the Se@DWNT is upshifted by 3 cm⁻¹ as a result of the Se atoms inside the tubes. Similar blueshift was experimentally detected of the G band (1064 nm excitation line) and reported for SWNT intercalated by electron acceptors (S, Se, and Te).⁹ The upshift caused of the rest of the filling materials is smaller than 3 cm⁻¹.

The Lorentzian components parameters acquired from the best 80 K G-band fit were used as initial conditions for every G-band fitting procedure applied for each sample at higher temperatures. As a result, for each filled DWNT sample obtained positions of the dominant G-band component are plotted as a function of temperature. In Fig. 3 the data are presented for the Se@DWNT, Te@DWNT, and compared to the empty DWNT.

In general, two main effects contribute to the phonon shift: purely thermal effect $(\partial\omega/\partial T)_V$ and volume related effect due to lattice expansion $(\partial\omega/\partial V)_T(\partial V/\partial T)_P$. The thermal expansion coefficient of the tube diameter and lattice constant for SWNT is very small and is experimentally determined by x-ray diffraction studies to be of the order of

TABLE I. Position and FWHM of the L3 and L4 components of the G-band and their integral intensity ratio and 80 K.

	L3		L4		I(L3)/I(L4)
	ω (cm ⁻¹)	Γ (cm ⁻¹)	ω (cm ⁻¹)	Γ (cm ⁻¹)	
Se@DWNT	1588	25	1604	32	6.3
Te@DWNT	1587	24	1603	28	6.8
PbI ₂ @DWNT	1586	23	1598	33	2.4
HgTe@DWNT	1586	24	1599	32	2.8
DWNT	1585	21	1595	31	1.5

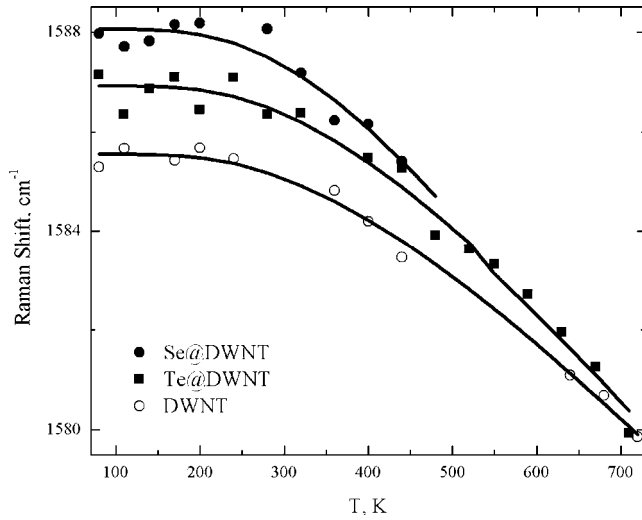


FIG. 3. Temperature dependence of L3 component of the G-band. The symbols represent the experimental data and the solid lines are the fit using Eq. (1).

0.15×10^{-5} 1/K and 0.75×10^{-5} 1/K, respectively, between 300 and 950 K.¹⁰ Therefore, the pure thermal effect, but not the volume expansion effect determined the temperature coefficients of the DWNT Raman bands.^{11,12} The temperature dependences of the frequency shift, $\Omega(T)$ of the L3 component of the G-band, as well as the D- and (2D)-bands, are analyzed in terms of the model developed by Klemens,¹³ Hart *et al.*,¹⁴ and Cowley¹⁵ and extended by Balkanski¹⁶ for anharmonic decay of optical phonons. The optical mode frequencies of the D- and G-bands approximately corresponds to Debye temperatures of 1870 K and 2280 K, respectively. Consequently, the occupation number for the equivalent harmonic oscillator is less than one for the temperature range of our investigation (80 to 700 K). Therefore, our considerations are always in the quantum mechanical limit of a classical harmonic oscillator. Also shown in Fig. 3 are the numerical fits to the data (solid curve) specified by the expression reflecting the contributions of the three-phonon processes (cubic anharmonicity),¹⁶ to the frequency shift

$$\Omega(T) = \omega_0 + C \left[1 + \frac{2}{e^x - 1} \right], \quad (1)$$

where $x = \hbar\omega_0/2k_B T$ if simple Klemens¹³ approximation is applied; k_B is the Boltzman constant; ω_0 is a fitting parameter corresponding to the quasi-harmonic frequency of the phonon

mode, and C is a fitting parameter related to the real part of the phonon's self energy. The values for ω_0 and C for the filled and empty DWNT are listed in Table II. The variations in the anharmonicity constant between the samples are not significant. The quasi-harmonic frequency, however is always higher than the quasi-harmonic frequency of empty DWNT. The highest shift is observed in the Raman spectra of Se@DWNT.

Raman D-band of the CNTs at around 1300 cm^{-1} is attributed to the bond-angle disorder in the graphitic layers induced by linking with sp^3 carbon atoms as a result of scattering in the presence of in-plane defects. The 2D-band (G'-band in some references) at around 2600 cm^{-1} is the overtone of the D-band.¹¹ D- and 2D-bands are not selective to the CNT diameter. Moreover, 2D-band is the second most intense feature in the DWNT Raman spectra after the G-band, and is observed even when the D-band is absent (in crystalline graphite). The D-band can be fitted with a single Lorentzian line shape (FWHM of around 60 cm^{-1}) in the range from 1220 to 1380 cm^{-1} . The 2D-band can be fitted with a single Lorentzian line shape in the range from 2450 to 2700 cm^{-1} with a FWHM of around 70 cm^{-1} . The integral intensity ratio of the D- and G-bands, $I(D)/I(G)$, is not more than 0.2. In the same time $I(2D)/I(G)$ varies between 0.8 and 1.0. According to earlier studies of graphene layers Raman spectroscopy can clearly distinguish a single layer, from a bilayer from few (less than 5) layers.¹⁷ Apparently, the 2D band is very sensitive to the stacking order of the graphene layers which is controlled by weak van der Waals forces (0.9% of the sp^2 carbon-carbon bond in the plane of the graphene¹⁸). In the same time, DWNT Raman spectra show a sharp 2D peak similar to that measured for graphene. Therefore, an inference can be made that the 2D-band can serve as an indicator for the strength of the van der Waals interactions between the nanotubes walls and the filling materials in case of filled DWNTs.

The temperature dependence of the D- and 2D-bands of filled and empty DWNT is presented in Fig. 4. The D-band temperature data are fit well using the cubic anharmonicity only, Eq. (1), see Fig. 4(a). The two fitting parameters obtained from each data set are summarized for all filling materials and compared with empty DWNT in Table II. On the other hand 2D band temperature dependence data sets can be fit well only if in addition to the cubic anharmonicity a quartic anharmonicity (four-phonon process) is taken into account, as earlier justified theoretically for the optical phonons

TABLE II. Fitting parameters of the temperature dependence data of the L3 component of the G-band, Eq. (1); D-band, Eq. (1); and 2D-band, Eq. (2).

	L3 (G-band)		D-band		2D-band	
	ω_0 (cm^{-1})	$C \pm 1$ (cm^{-1})	ω_0 (cm^{-1})	C (cm^{-1})	C (cm^{-1})	D (cm^{-1})
Se@DWNT	1602	-14	1314	-9 ± 1	-28.0 ± 0.6	5.0 ± 0.4
Te@DWNT	1600	-13	1312	-11 ± 1	-26.5 ± 0.4	4.5 ± 0.2
PbI ₂ @DWNT	1598	-12	1310	-8.0 ± 0.5	-21.5 ± 0.5	3.0 ± 0.2
HgTe@DWNT	1601	-15	1307	-6.0 ± 0.5	-19.5 ± 0.5	3.5 ± 0.2
DWNT	1596	-11	1305	-6.0 ± 0.5	-19.5 ± 0.5	3.0 ± 0.5

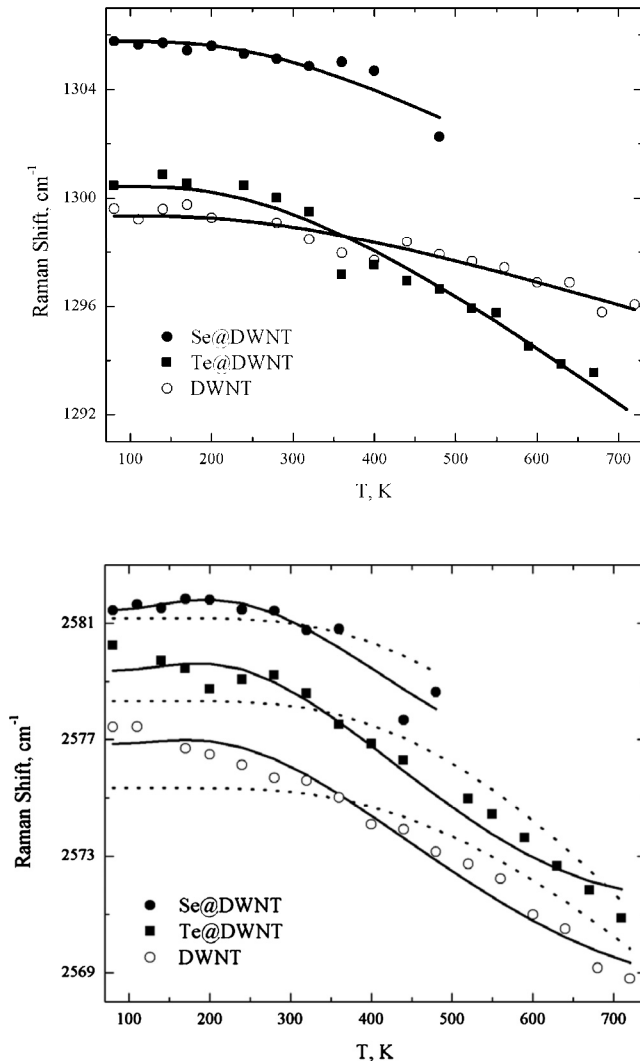


FIG. 4. (a) Temperature dependence of the D-band. The symbols represent the experimental data and the solid lines are the fit using Eq. (1). (b) Temperature dependence of the 2D-band. The symbols represent the experimental data and the solid lines are the fit using Eq. (2), the dashed line represent the fit using Eq. (1).

of Silicon by Balkanski *et al.*¹⁶ Figure 4(b) shows the numerical fits to the data (solid curves) specified by the expression reflecting the contributions of the three-phonon (cubic anharmonicity) and four-phonon processes (quartic anharmonicity) to the frequency shift¹⁶ applied to the second order band

$$\Omega(T) = 2\omega_0 + 2C \left[1 + \frac{2}{e^x - 1} \right] + 2D \left[1 + \frac{3}{e^y - 1} + \frac{3}{(e^y - 1)^2} \right], \quad (2)$$

where x , ω_0 , and C are explained above, $y = \hbar\omega_0/3k_B T$, if simple Klemens¹³ approximation for a quartic anharmonicity, and D is a third fitting parameter corresponding to the contribution of the quartic anharmonicity. In the above expression, ω_0 , C , and D can be associated with either one of the two identical optical phonons contributing to the second order 2D band. The values of the fitting parameters for each curve are listed in Table II. The ratio D/C is less than one, in

accordance to the expectation that the four-phonon processes have less contribution compared to the three-phonon processes. For the fitting procedure of the temperature dependence of the 2D band the quasi-harmonic frequency obtained from the temperature dependence of the D-band fit was used and fixed. Therefore, again there were only two fitting parameters, the anharmonicity constants C and D .

In all data sets there is a well expressed tendency for the filled DWNT to have larger anharmonicity constants in comparison to the empty DWNT sample. In agreement with the G-band study, the quasi-harmonic frequencies listed in Table II are smallest for the empty DWNT (1305 cm^{-1}) and largest for the Se@DWNT (1314 cm^{-1}). In addition, up to 40% increase in the absolute value of the cubic anharmonicity parameter is observed, suggesting substantially stronger contribution to the nanotube phonon decay due to the phonon-phonon interaction between the nanotubes and the filling material. It is evident that more pronounced anharmonicity is accompanied by a larger quasi-harmonic frequency of the specific phonon mode. All parameters are compared to those of empty DWNTs.

In order to estimate the relative strength of the van der Waals interaction between the tube walls and the filling material we considered a simple one dimensional arrangement of two masses (one being the carbon atom, m_c , from the tube wall, and the other being the atom from the filling material, m_f) connected with three Hooke's springs.¹⁹ Each spring constant is proportional to the corresponding bond strength. The spring connected to m_c represents the C-C bond in the CNT; the middle spring, k_2 , represents the interaction between the tube wall and the filling material, and finally, the third spring, k_3 represents the bond in the filling material. Solving the equations of motions for the two masses and finding the normal modes of the system, ω_o , allowed us to express the relative strength of the middle spring, $a_2 = k_2/k_1$ as

$$a_2 = \frac{\left(\frac{\omega_0^2}{\omega_{0\text{DWNT}}^2} - 1 \right) \times \left(\frac{\omega_0^2}{\omega_{0\text{DWNT}}^2} b - a_3 \right)}{\left(\frac{\omega_0^2}{\omega_{0\text{DWNT}}^2} - 1 \right) + \left(\frac{\omega_0^2}{\omega_{0\text{DWNT}}^2} b - a_3 \right)}, \quad (3)$$

where $\omega_{0\text{DWNT}}^2 = k_1/m_c$; $a_3 = k_3/k_1$; and $b = m_f/m_c$.

Furthermore, taking into account that

$$\left(\frac{\omega_0^2}{\omega_{0\text{DWNT}}^2} - 1 \right) \ll \left(\frac{\omega_0^2}{\omega_{0\text{DWNT}}^2} b - a_3 \right).$$

Equation (3) can be further approximated to a simple expression that can be used for a relative estimate of the strength of interaction between the tube wall and the filling material

$$a_2 \approx \frac{\omega_0^2 - \omega_{0\text{DWNT}}^2}{\omega_{0\text{DWNT}}^2}. \quad (4)$$

Substituting the quasi-harmonic frequencies found from the temperature fit for each filling material, ω_0 (see Table II), and using the quasi-harmonic frequency obtained for the empty DWNT $\omega_{0\text{DWNT}} = 1305 \text{ cm}^{-1}$, the relative bond strength between the nanotubes wall and the filling material

TABLE III. Quasiharmonic frequency and estimated relative strength of the van der Waals interaction for each material as percent from the C–C bond in the plane of a graphene sheet

	ω_0 (cm^{-1})	a_2 (%)
Se@DWNT	1314	1.4
Te@DWNT	1312	1.1
PbI ₂ @DWNT	1310	0.8
HgTe@DWNT	1307	0.3

is estimated. The results are summarized in Table III. It can be seen that van der Waals interaction between the Se and Te and the tube walls is stronger than the interaction between the graphene layers in graphite. On the other hand, it appears that HgTe interaction is considerably weaker.

The experimental data reported in this study support strongly the theoretical models²⁰ utilizing the equation of motion method where the phonon Green's function for the nanotube has been calculated taking into account of the phonon–phonon interaction and the electron–phonon interaction within the random phase approximation. It was established that stronger phonon–phonon interaction between the localized phonon of the filling material and nanotubes would lead to higher frequency shift in the main resonance mode of the nanotubes.

IV. CONCLUSION

Systematic comparative experimental study (80–700 K) of the most prominent Raman bands of Se@DWNT, Te@DWNT, PbI₂@DWNT, and HgTe@DWNT in powder form was carried out. The G-band and D-band temperature shifts are satisfactorily described with cubic anharmonicity only. The interactions between the filling material and the tube walls have been shown not to be important for the G-band Raman spectra. The 2D-band temperature dependence can be fit only if in addition to the cubic anharmonicity, a quartic anharmonicity is included. In addition, the anharmonicity analysis of the temperature data allowed us to determine the quasiharmonic frequency for the disorder induced Raman mode which we used to estimate the relative strength of interaction between the CNT walls and the filling materials. The interaction decreases in the following order:

Se@DWNT; Te@DWNT; PbI₂@DWNT, and HgTe@DWNT. It was established that the anharmonicity parameters of the D- and 2D-bands decrease in the same order too. The 2D band proved to be the most sensitive indicator for the presence and the type of the filling material in the Raman spectrum of DWNTs.

ACKNOWLEDGMENTS

M.S. wants to thank Professor H. Sendov and Professor G. Ruppreiter for the helpful discussions. E.F. thanks Dr. J. Sloan and L. Datas for the HRTEM. The work is done with the ARL financial support under Grant No. W911NF-09-2-0004.

- ¹E. Flahaut, J. Sloan, S. Friedrichs, A. I. Kirkland, K. S. Coleman, V. C. Williams, N. Hanson, J. L. Hutchison, and M. L. H. Green, *Chem. Mater.* **18**, 2059 (2006).
- ²R. Carter, J. Sloan, A. I. Kirkland, R. R. Meyer, P. J. D. Lindan, G. Lin, M. L. H. Green, A. Vlandas, J. L. Hutchison, and J. Harding, *Phys. Rev. Lett.* **96**, 215501 (2006).
- ³E. Flahaut, R. Bacsa, A. Peigney, and Ch. Laurent, *Chem. Commun. (Cambridge)* **2003**, 1442.
- ⁴M. Sendova, L. Datas, and E. Flahaut, *J. Appl. Phys.* **105**, 094312 (2009).
- ⁵M. Sendova and E. Flahaut, *J. Appl. Phys.* **103**, 024311 (2008).
- ⁶A. Bassil, P. Puech, L. Tubery, W. Bacsa, and E. Flahaut, *Appl. Phys. Lett.* **88**, 173113 (2006).
- ⁷<http://www.photon.t.u-tokyo.ac.jp/~maruyama/kataura/kataura.html>
- ⁸A. Jorio, A. G. Souza Filho, G. Dresselhaus, M. S. Dresselhaus, A. K. Swan, M. S. Unlü, B. B. Goldberg, M. A. Pimenta, J. H. Hafner, C. M. Lieber, and R. Saito, *Phys. Rev. B* **65**, 155412 (2002).
- ⁹M. V. Chernysheva, E. A. Kiseleva, N. I. Verbitskii, A. A. Eliseev, A. V. Lukashin, Y. D. Tretyakov, S. V. Savilov, N. A. Kiselev, O. M. Zhigalina, A. S. Kumskov, A. V. Krestinin, and J. L. Hutchison, *Physica E (Amsterdam)* **40**, 2283 (2008).
- ¹⁰Y. Maniwa, R. Fujiwara, H. Kira, H. Tou, H. Kataura, S. Suzuki, Y. Achiba, E. Nishibori, M. Takata, M. Sakata, A. Fujiwara, and H. Suenmatsu, *Phys. Rev. B* **64**, 241402(R) (2001).
- ¹¹M. S. Dresselhaus and P. C. Eklund, *Adv. Phys.* **49**, 705 (2000).
- ¹²L. Ci, Z. Zhou, L. Song, X. Yan, D. Liu, H. Yuan, Y. Gao, J. Wang, L. Liu, W. Zhou, G. Wang, and S. Xie, *Appl. Phys. Lett.* **82**, 3098 (2003).
- ¹³P. G. Klemens, *Phys. Rev.* **148**, 845 (1966).
- ¹⁴T. R. Hart, R. L. Aggarwal, and B. Lax, *Phys. Rev. B* **1**, 638 (1970).
- ¹⁵R. A. Cowley, *J. Phys. (Paris)* **26**, 659 (1965).
- ¹⁶M. Balkanski, R. F. Wallis, and E. Haro, *Phys. Rev. B* **28**, 1928 (1983).
- ¹⁷A. C. Ferrari, J. C. Meyer, V. Scardaci, C. Casiraghi, M. Lazzeri, F. Mauri, S. Piscanec, D. Jiang, K. S. Novoselov, S. Roth, and A. K. Geim, *Phys. Rev. Lett.* **97**, 187401 (2006).
- ¹⁸M. Schabel and J. L. Martins, *Phys. Rev. B* **46**, 7185 (1992).
- ¹⁹To be published.
- ²⁰S. M. Bose, S. N. Behera, S. N. Sarangi, and P. Entel, *Physica B* **351**, 129 (2004).